Bistatic remote sensing of the atmosphere and surface using GNSS occultations signals

Alexander Pavelyev[1], Kefei Zhang[2], Stanislav Matyugov[1], Yuei-An Liou[4], Oleg Yakovlev[1], Igor Kucherjavenkov[1], Carl Wang[2], Yuriy Kuleshov[2]

[1]Institute of Radio Engineering and Electronics, Russian Academy of Sciences, Fryazino, Russia E-mail: pvlv@ms.ire.rssi.ru

[2]School of Mathematical and Geospatial Sciences, RMIT University, Melbourne, Australia kefei.zhang@rmit.edu.au

[3]Center for Space and Remote Sensing Research (CSRSR), National Central University, Jhongli, Taiwan yueian@csrsr.ncu.edu.tw

GNSS R'10 October 22 Barcelona Spain

RMIT UNIVERSITY
GEOSPATIAL SCIENCE

Content

(i) Introduction. Some historical remarks

(ii)Conditions of detection of reflected signals from space by RO receiver are analyzed. An analytical model is introduced for ray tracing of the direct and reflected signals. The phase delay, Doppler shift, reflection coefficient, reflectivity cross-section, of reflected signals are obtained in analytical forms.

(iii) Connection between the amplitude and phase variations of the radio signals propagating in the satellite-to-satellite links is obtained. The innovative eikonal acceleration technique is described for application to the analysis of the direct and reflected signals.

(iv) MIR/GEO measurements data are described (wavelengths 2 and 32 cm).

Radio occultation and bistatic radio location at the satellite-to-satellite links orbital station “MIR” – Geostationary satellites at wavelengths 32 and 32 cm (~ 89 sessions during the period 1989- 1998).

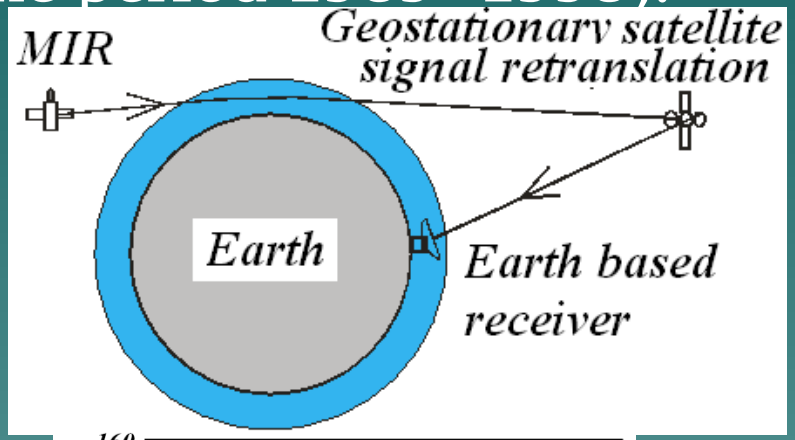

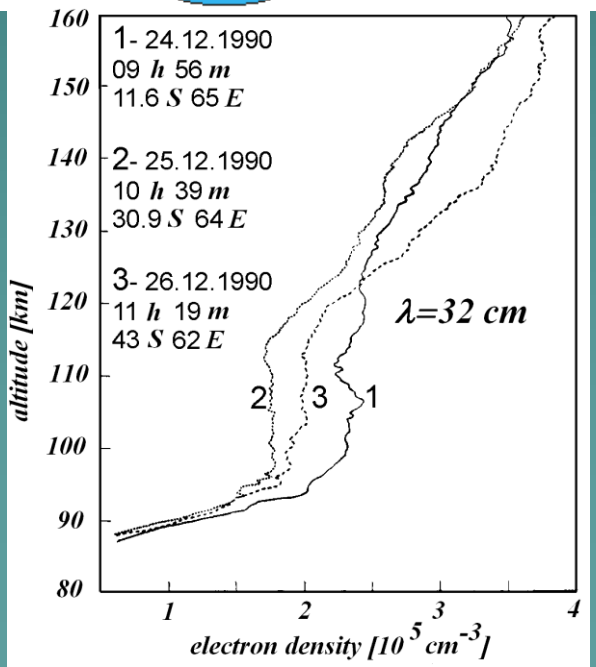

Variations of the total water vapor absorption of centimeter waves in the troposphere (Yakovlev et al., 1993)

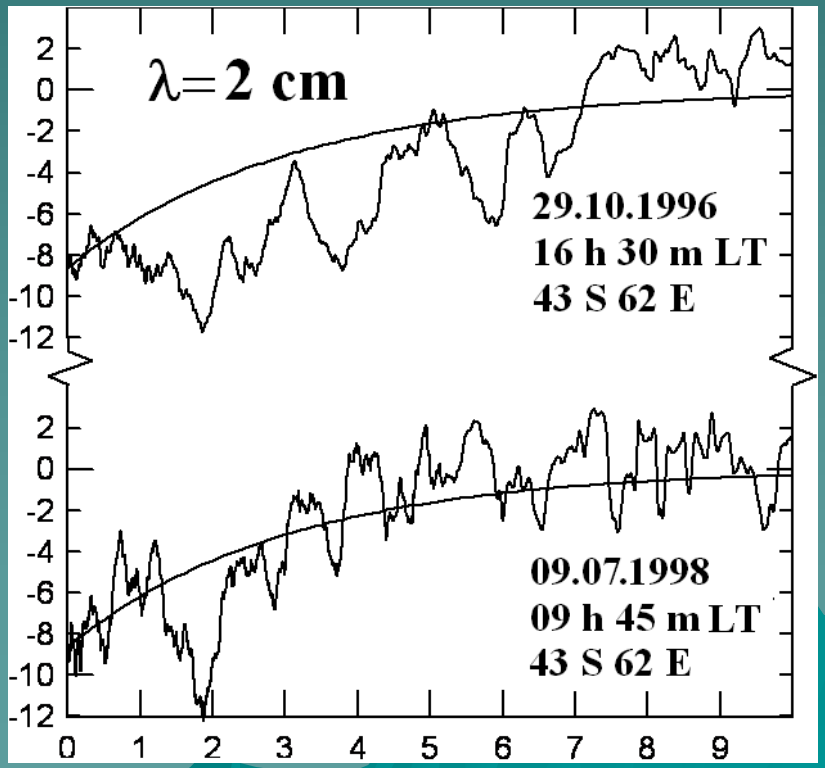

Bistatic radio location of the Earth surface from space

- 1989 – 1998: Registration of the reflected signals from the Earth surface in the decimeter and centimeter range in the satellite-to-satellite communication link. IRE RAS.
- Milekhin O.E., A.I.Kucherjavenkov, A.G. Pavelyev (1986), The analysis of possibility of bistatic radiolocation of Earth using satellite-to-satellite link, *Issledovania Zemli iz kosmosa*, 4, 86-94. (In Russian).
- Belan V.N. et al. Bistatic investigations of the phase and amplitude variations of reflections from the Earth surface. *J. Commun. Techn. Electron.*, *33*(4), 826-833, 1988.
- Rubashkin S.G., A.G. Pavelyev, O.I. Yakovlev, A.I. Kucherjavenkov, A.I. Sidorenko, A.I. Zakharov (1993), Bistatic reflection of radio waves from the sea surface from data of two satellites, *J. Commun. Techn. Electron.*, *38*(9), 447-453.
- Pavelyev A.G., A.V.Volkov, A.I. Zakharov, S.A. Krytikh, A.I.Kucherjavenkov: Bistatic radar as a tool for Earth observation using small satellites. Acta Astronautica 1996, V.39. No.9-12. P.721-730.
- Pavelyev A. G., A. I. Zakharov, A. I. Kucherjavenkov,A.I. Sidorenko, I. L. Kucherjavenkova, and D. A. Pavelyev (1997), The features of propagation of radio wave reflected from terrestrial surface at small elevation angles on radio telecommunication link low orbital satellite-GEO, *J. Commun. Technol. Electron.*, 42(1), 51-57.

Bistatic radio location: analytical model of eikonals $S(p_d)$, $S(p_r)$ and refractive attenuations $X(p_d)$, $X(p_r)$ of direct and reflected signals

$$S_r = \sqrt{R_L^2 - p_r^2} + \sqrt{R_G^2 - p_r^2} - 2\sqrt{n^2(a)a^2 - p_r^2} + 2p_r\xi_r(p_r) + 2\kappa_r(p_r) - S_s(p_s)$$

$$S_d = \sqrt{R_L^2 - p_d^2} + \sqrt{R_G^2 - p_d^2} + p_d\xi_d(p_d) + \kappa_d(p_d) - S_s(p_s)$$

$$S_s(p_s) = \sqrt{R_L^2 - p_s^2} + \sqrt{R_G^2 - p_s^2}$$

$$\xi_{d,r}(p_{d,r}) = -\frac{d\kappa_{d,r}(p_{d,r})}{dp_{d,r}}$$

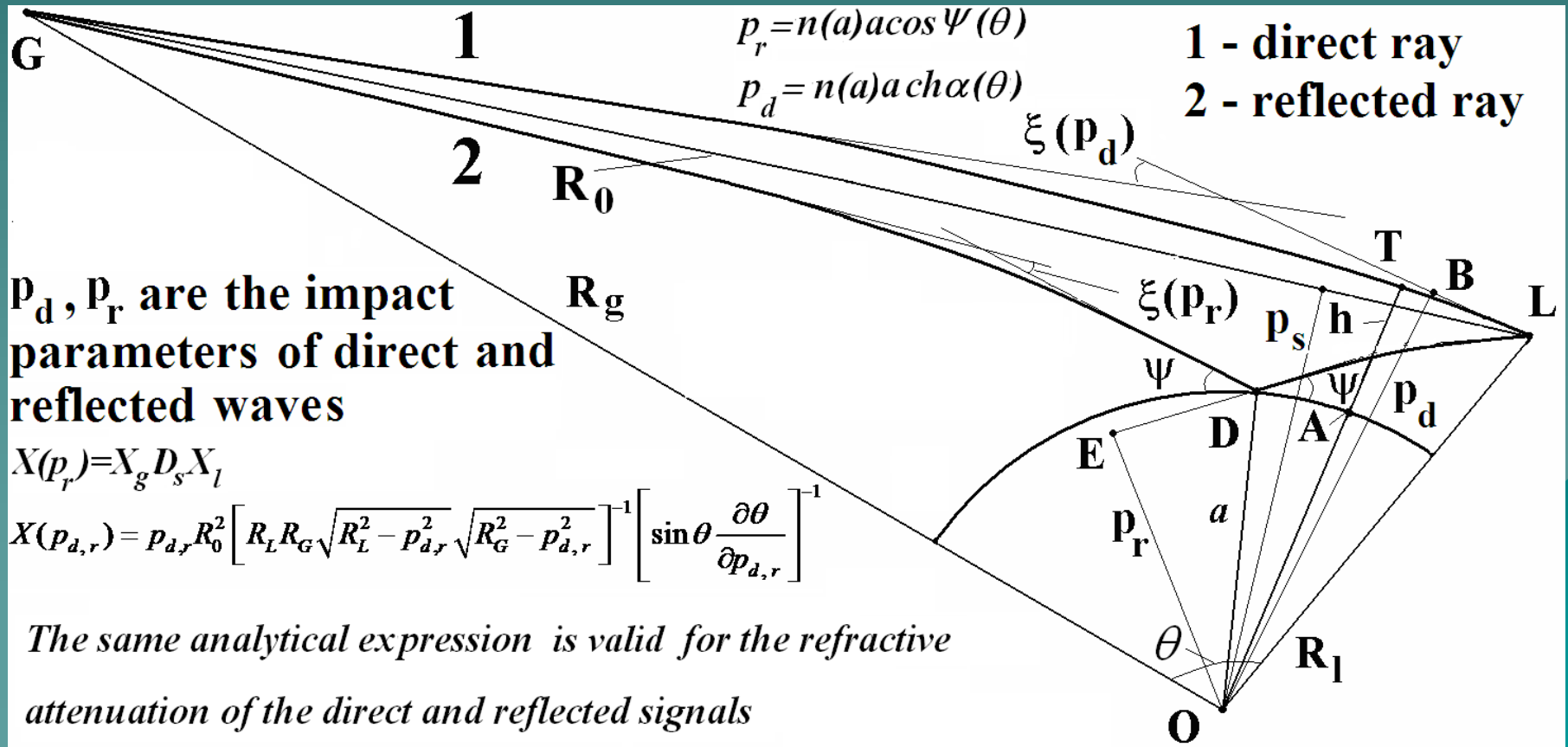

Ray tracing: model of the refractivity (left) and vertical gradient of refractivity (right) corresponding the direct and reflected signals in the atmosphere (Pavelyev et al., 1996, Acta Astronautica)

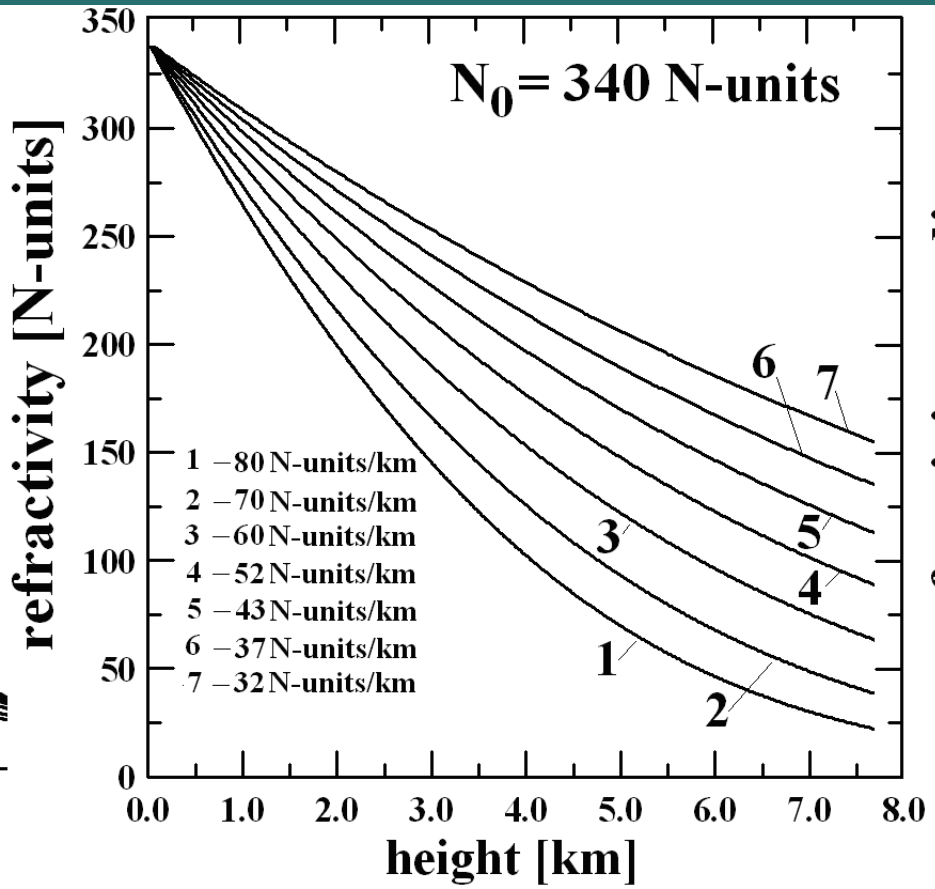

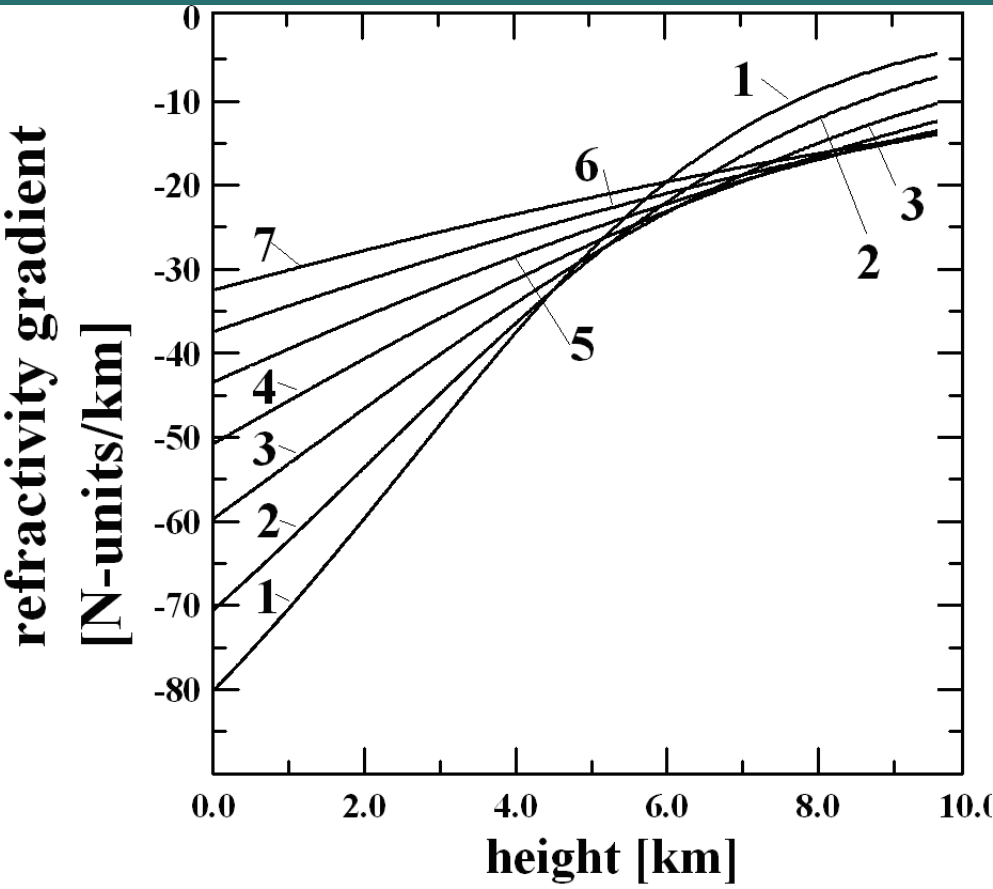

Ray tracing: the refractive angles related to the reflected (curves 1-7) and direct (curves 8-14) signals (left) and the relationship between the arguments of the impact parameters α, ψ (right) related to the direct and reflected signals. The magnitudes α, ψ have been calculated for the same values of the central angle θ.

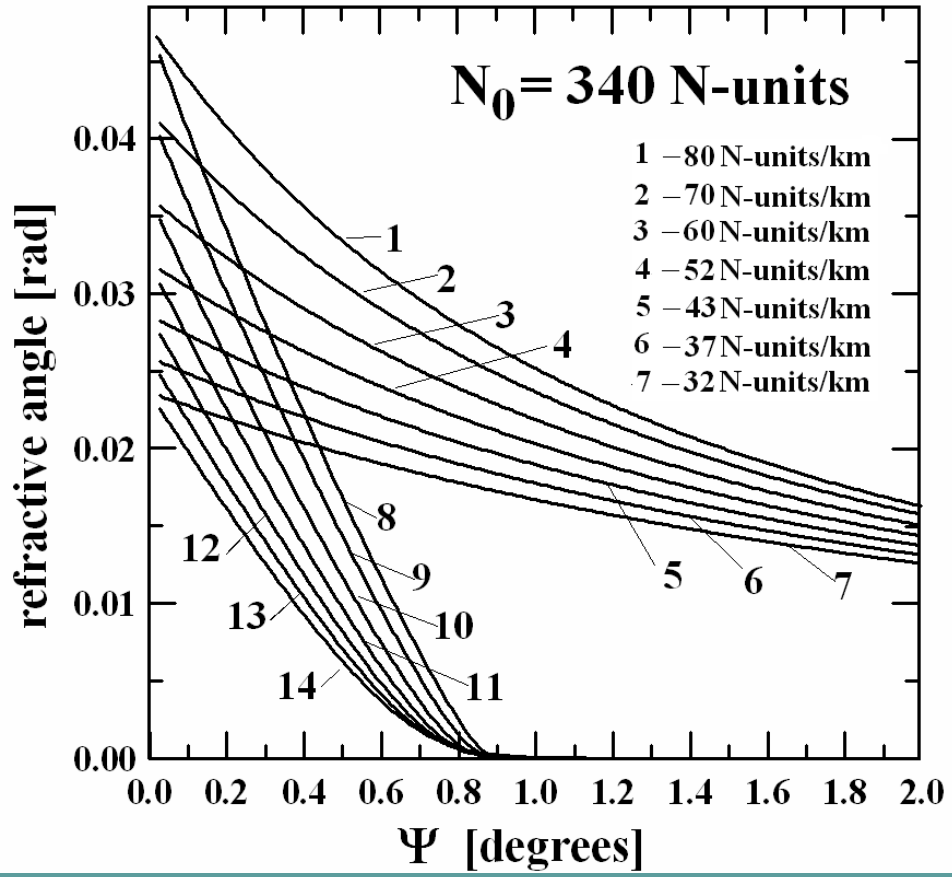

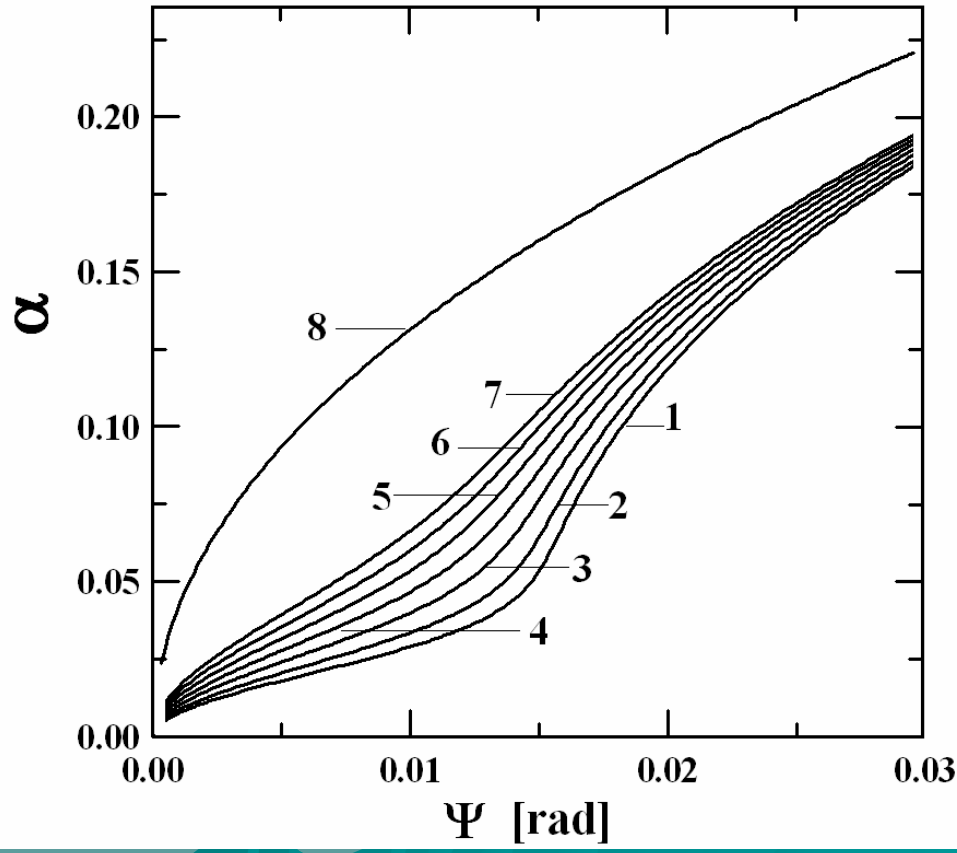

Ray tracing: atmospheric part of difference of the phase delays of the reflected and direct signals S_r-S_d as a function of the altitude of the ray perigee h and vertical gradient of refractivity for magnitudes of near-surface refractivity N_0 equal to 340 N-units (left) and 480 N-units (right), respectively. At the altitudes below 20 km the reflections can be detected because they are in the same correlation chip with direct signal.

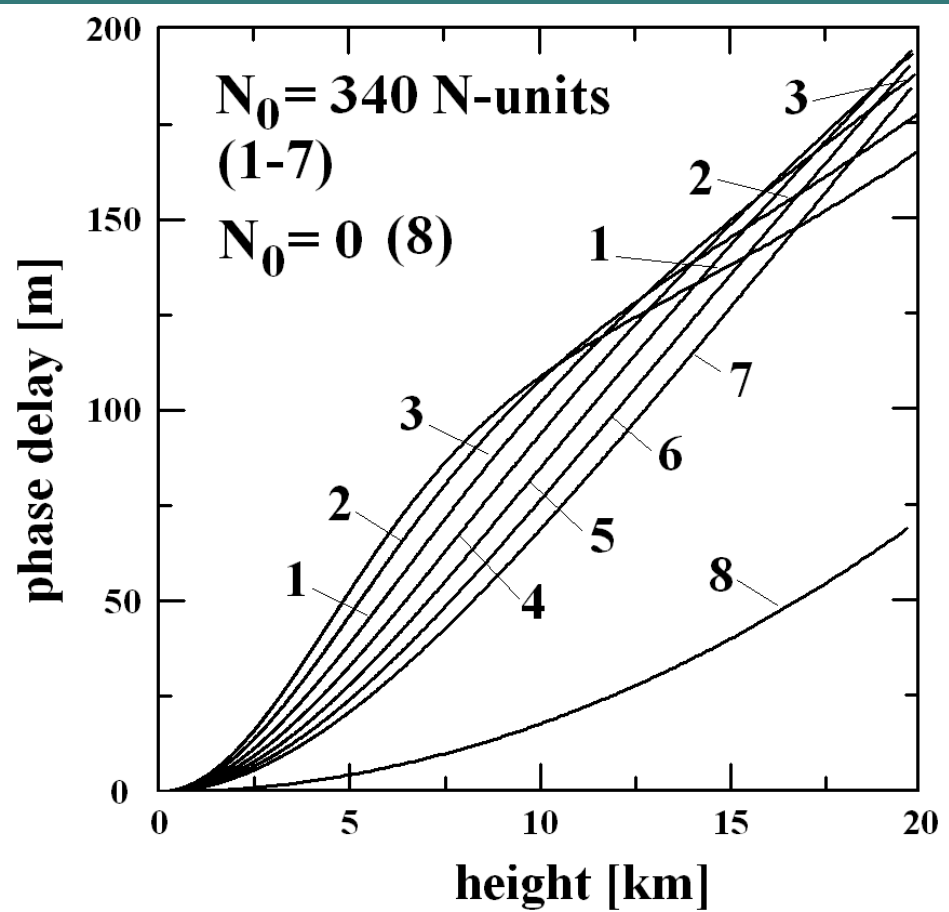

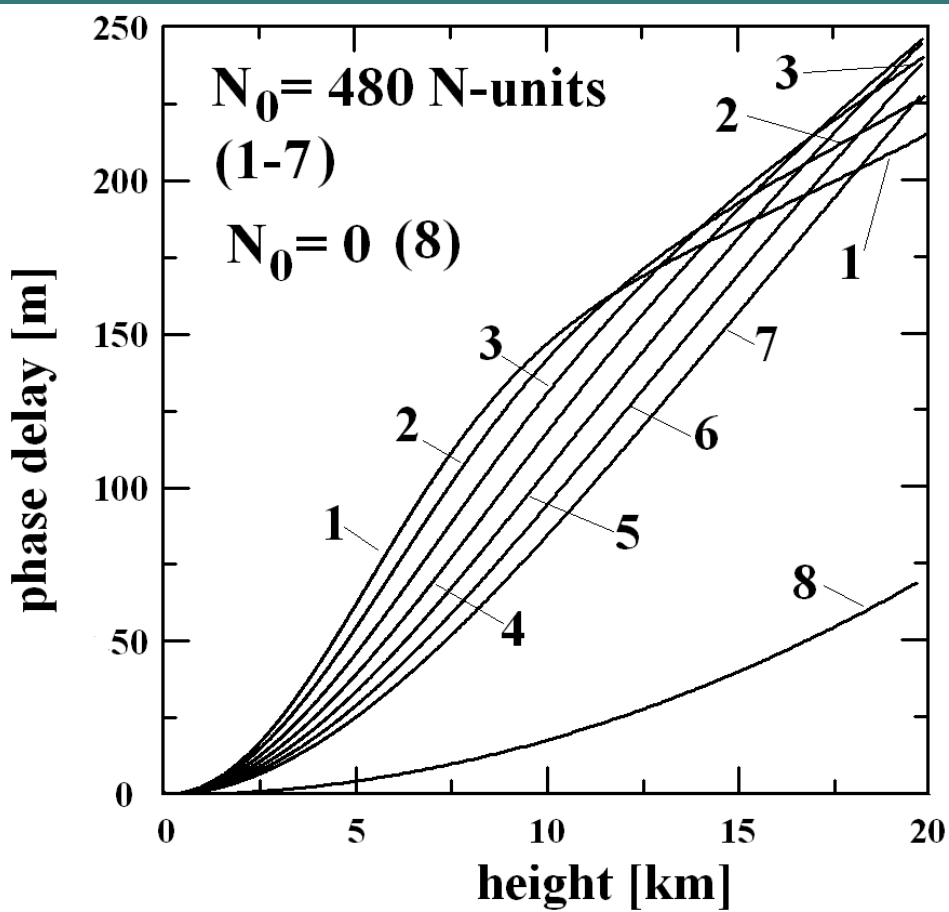

Ray tracing: difference of the Doppler shifts of the reflected signal and direct signals as a function of the grazing angle (right) and the dependence of the grazing angle on the height (left).

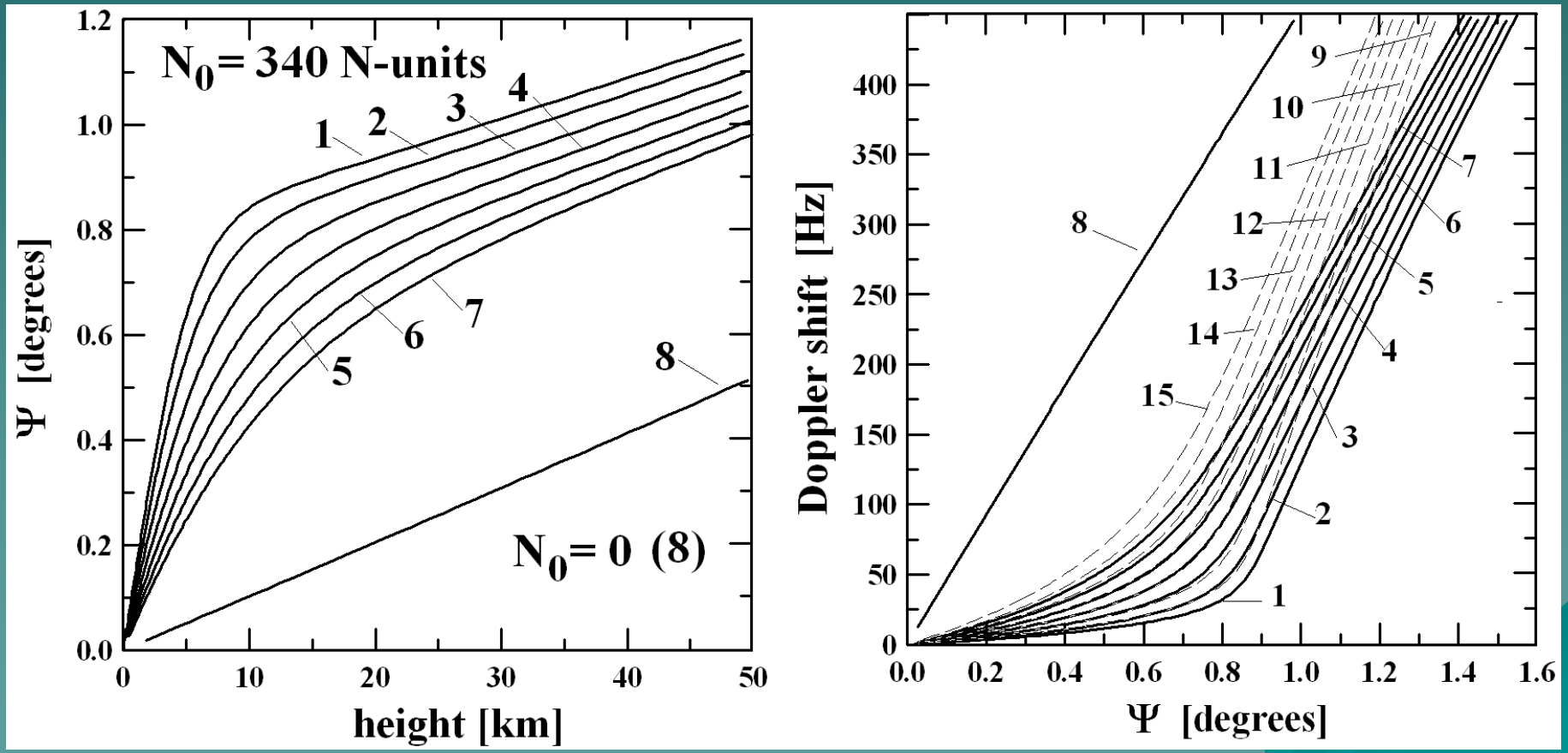

Reflection coefficient η^2 (ψ) for the case of the right hand (RHCP) and left hand (LHCP) circular polarizations of a GPS RO receiving antenna.

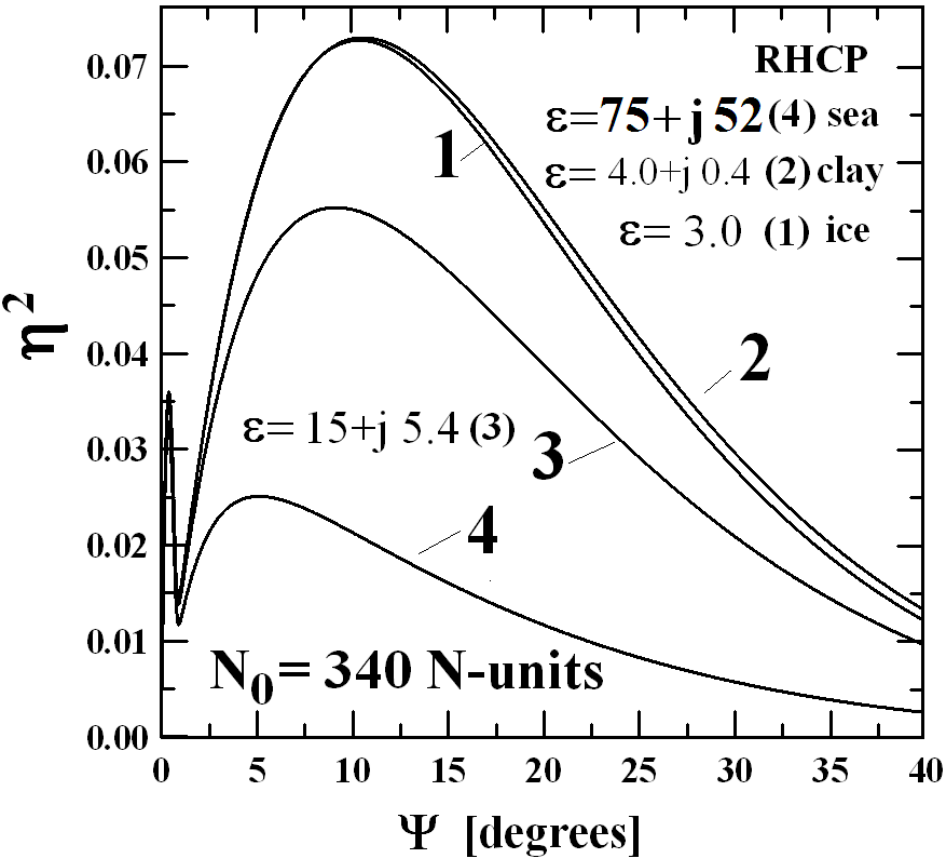

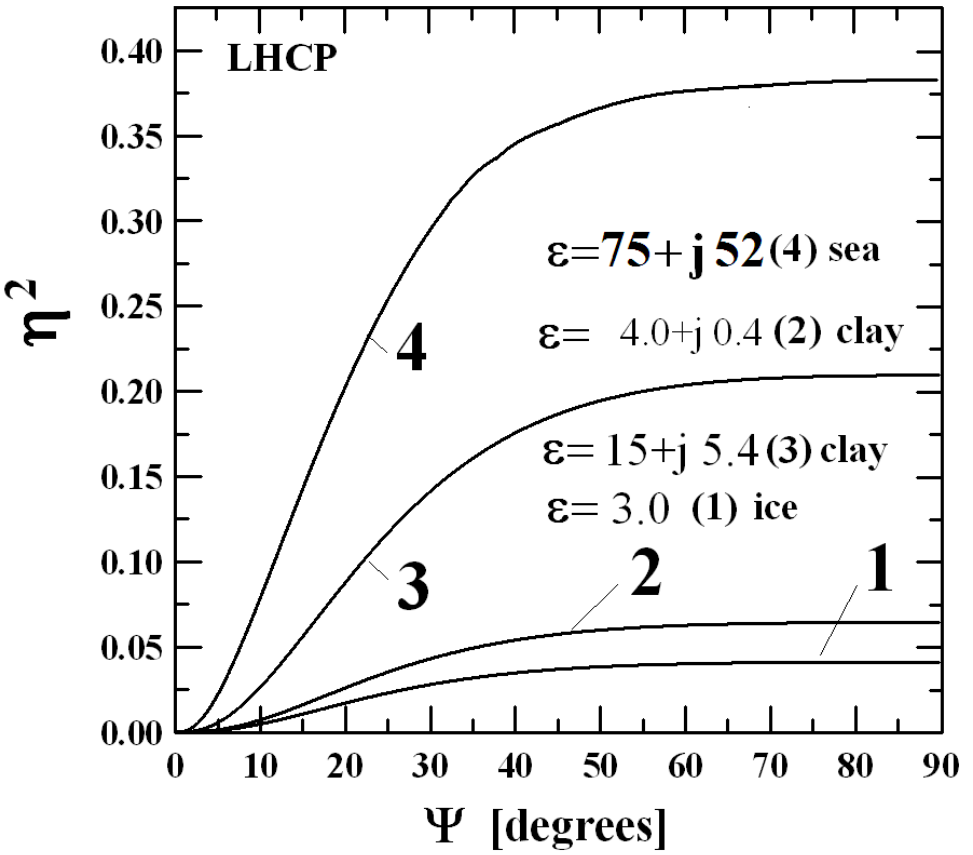

Connection between the amplitude and eikonal in the RO and bistatic scheme

(Liou and Pavelyev, GRL, 2006; Pavelyev et al., JGR, 2007). The eikonal acceleration has the same importance for RO data analysis as the Doppler frequency. It allows one to recalculate the phase data to the refractive attenuation. This connection opens the independent way to estimate absorption from ratio of the refraction attenuations found from the amplitude and phase data.

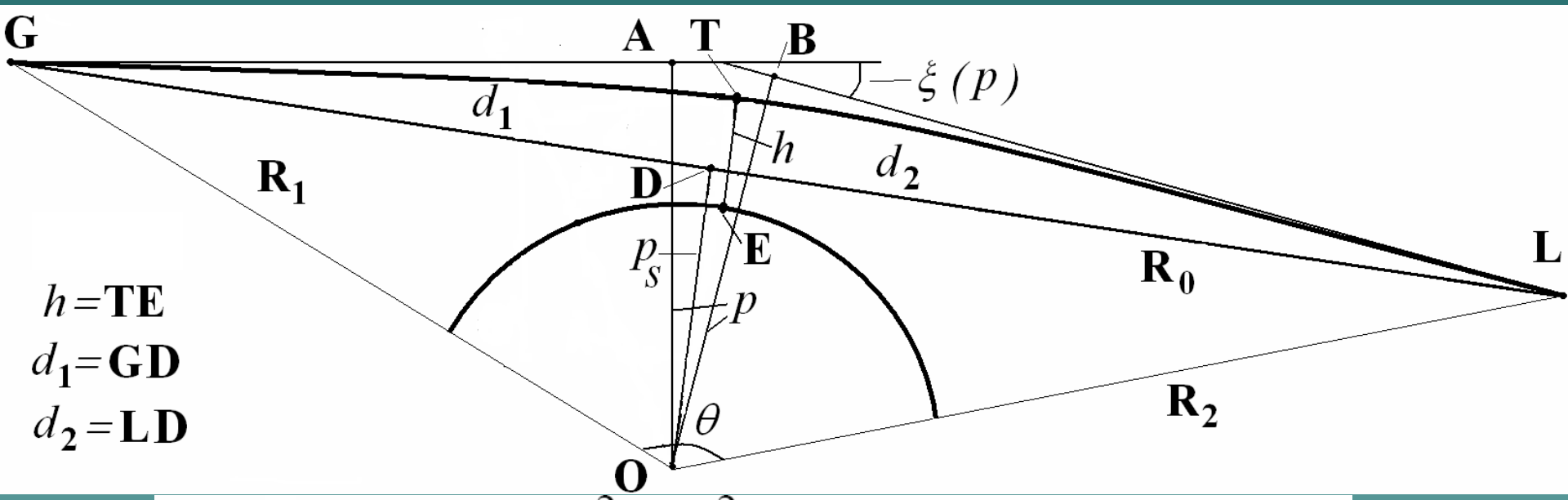

$1 - X_p(t) = ma$, $a = d^2S/dt^2$, a *is the eikonal acceleration*

$X = A^2/A_0^2$ *is the intensity attenuation* (*refractive attenuation plus absorption*)

$m = d_1 d_2 / R_0 (dp_s/dt)^{-2}$, $F = dS/dt$ *is the Dopler frequency*

$X_p(t)$ *is the refractive attenuation*

Experimental evidences of connection between the refractive attenuations X_a and X_p retrieved from the FORMOSAT-3 amplitude and phase RO data (neutral atmosphere and lower ionosphere). The antenna's amplitude diagram influence is seen in the intensity data.

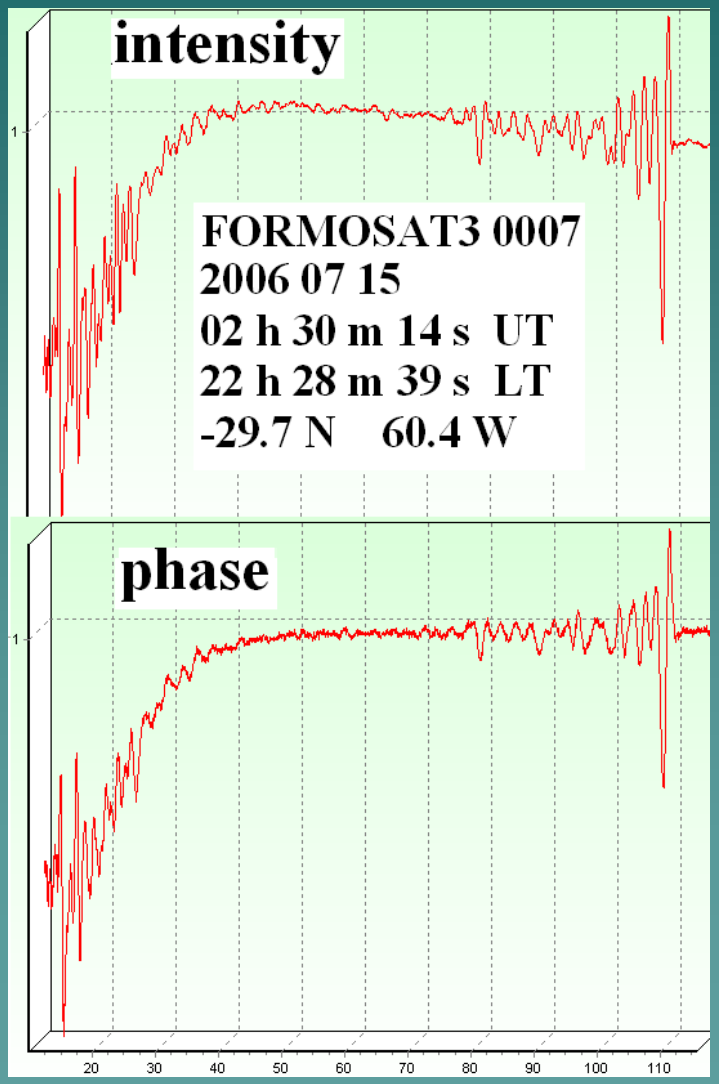

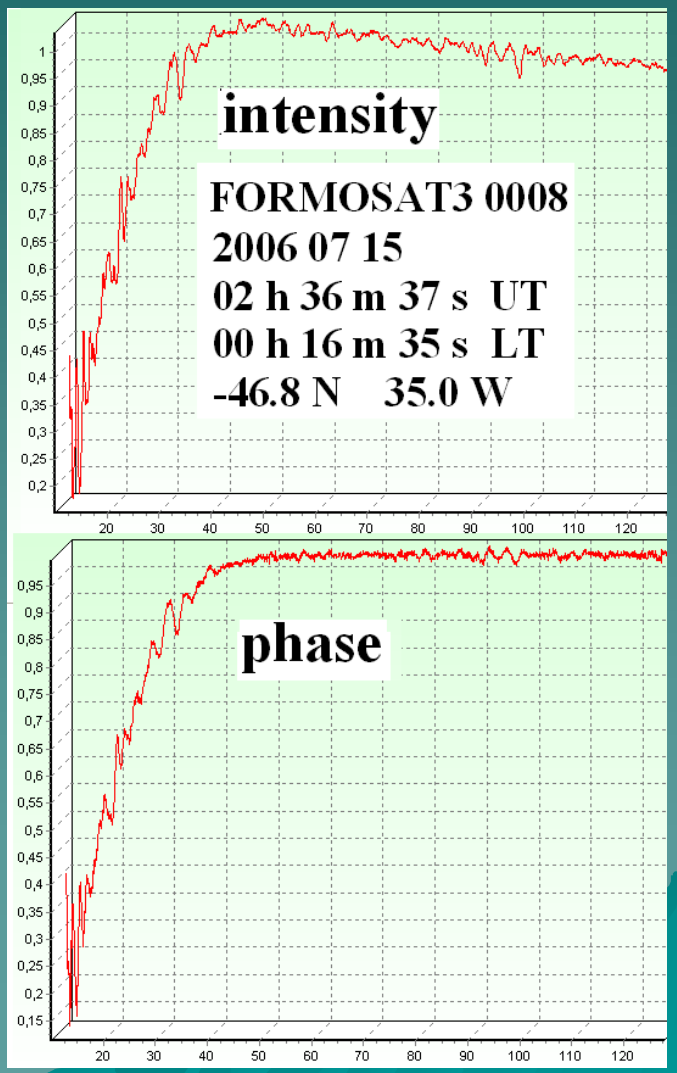

Experimental evidences of connection between the refractive attenuations X_a and X_p and derivative of the Doppler frequency on time obtained from RO data relevant to the Venus ionosphere (Venera-15 mission, 1983) (Pavelyev et al., GRL, 2009).

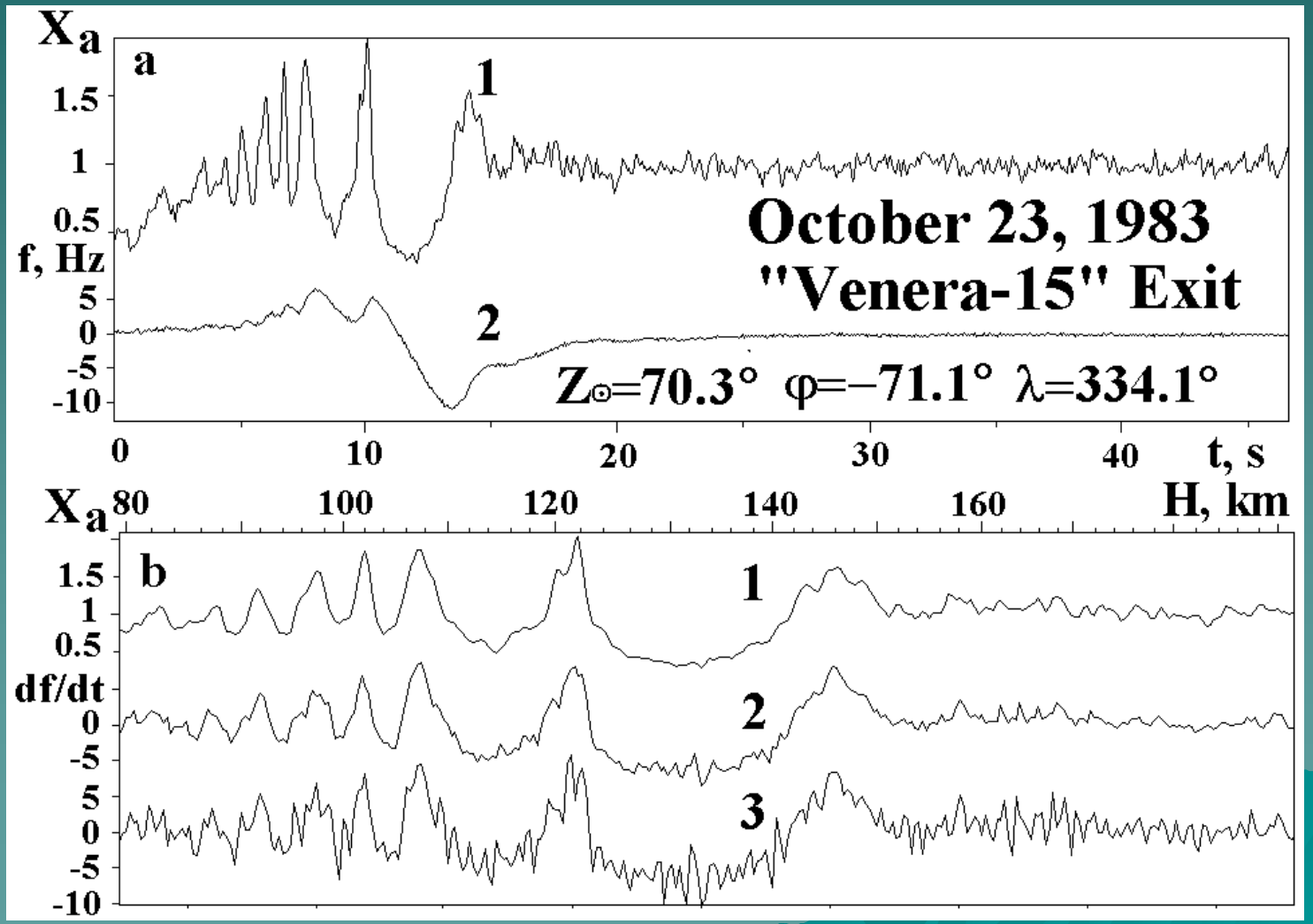

A possibility to measure absorption of radio waves by comparison of the amplitude and phase parts of the GPS radio-holograms (e.g., two events). Curves 1 and 2 describe attenuations obtained from the amplitude and phase data, respectively. Curves 3 and 4 indicate theoretical dependence of the refraction attenuation with absorption and refraction attenuation, correspondingly (Pavelyev et al., GRL, 2009).

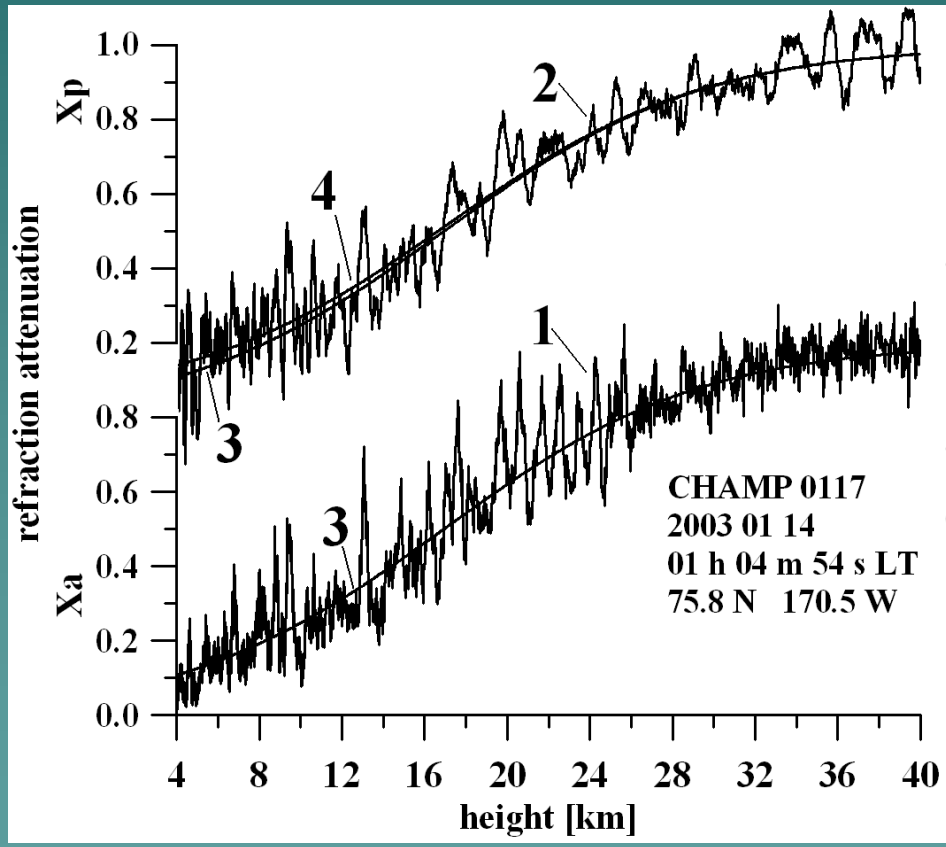

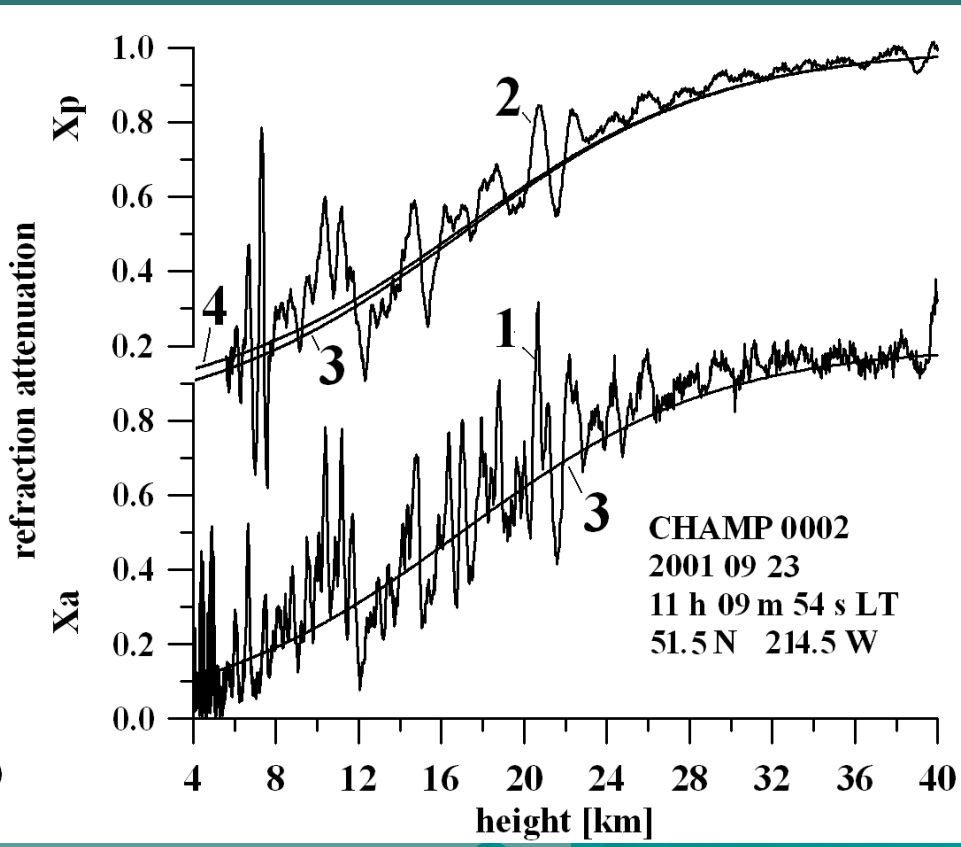

Curves 1 - 5 indicate experimental dependence of refraction attenuation calculated from amplitude and phase data. Curves 6-10 demonstrate experimental dependence of the integral absorption. Curves A,B indicated the theoretical dependence of the refraction attenuation and integral absorption (Pavelyev et al., GRL, 2009)

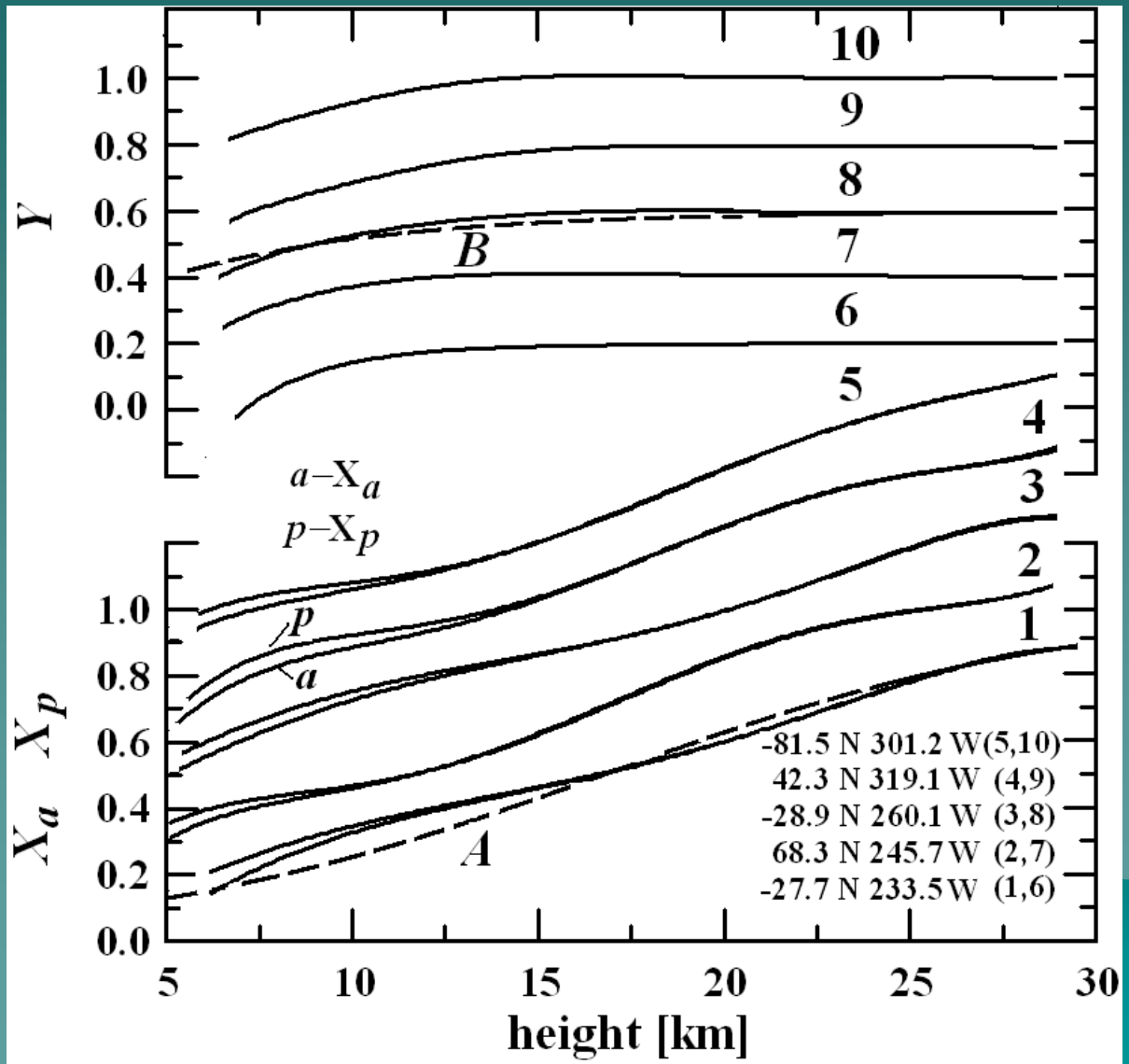

Generalization to the case of reflections from the Earth's surface. Connection between the refractive attenuations X_d, X_r and derivative of the difference of the Doppler frequencies ΔF of the direct and reflected signals with respect to time (Pavelyev et al., 2010, Radio Science under review)

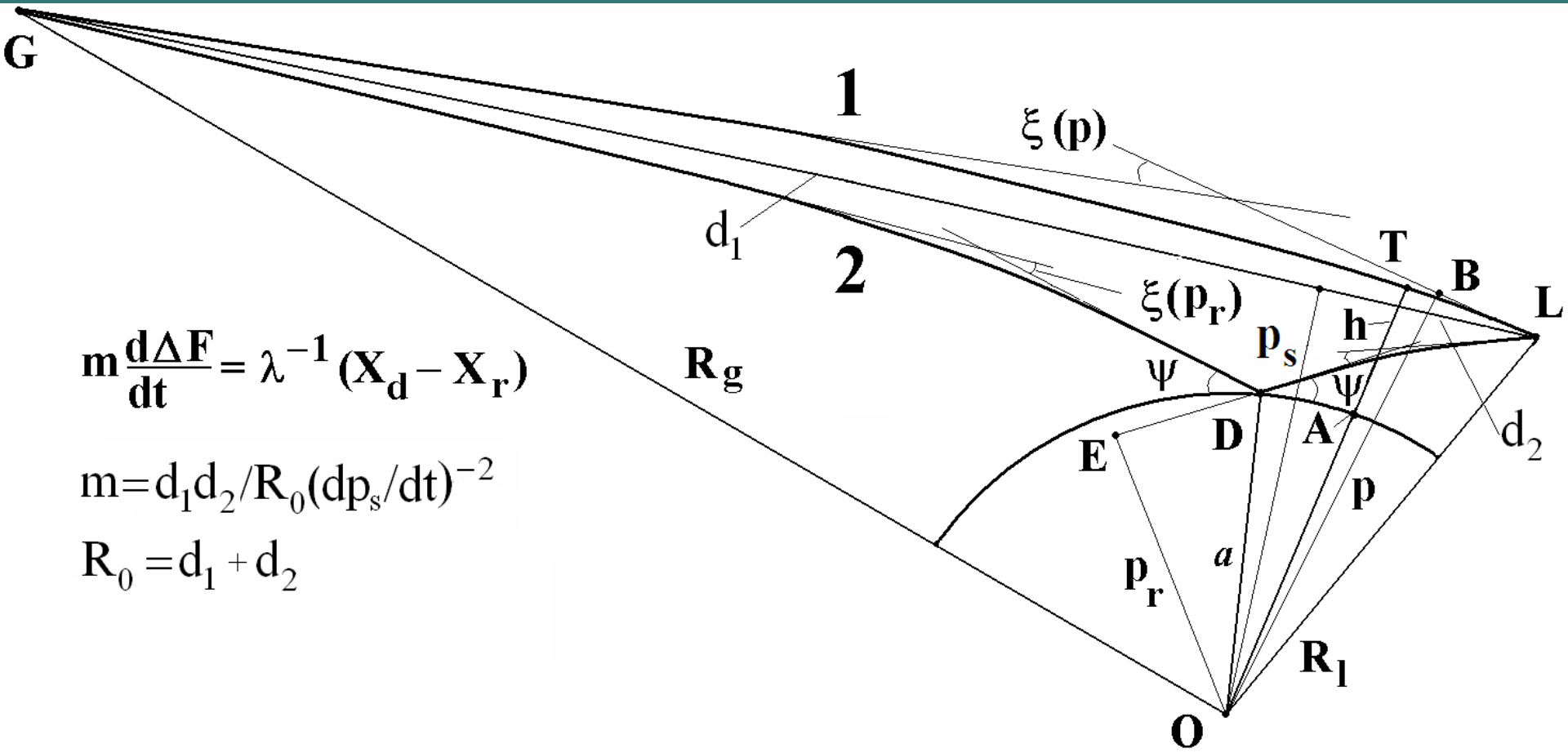

$$m\frac{d\Delta F}{dt} = \lambda^{-1}(X_d - X_r)$$

$$m = d_1 d_2 / R_0 (dp_s/dt)^{-2}$$

$$R_0 = d_1 + d_2$$

Revealing the reflection from the sea surface from data of Micro-Lab-1 (λ=19 cm) and MIR-GEO (λ=32 and 2 cm) (Pavelyev et al., 1996). Investigation by radio-holographic focused synthetic aperture (RHFSA) method the reflected signal from data of GPS-MET (Igarashi, Pavelyev et al., 2001).

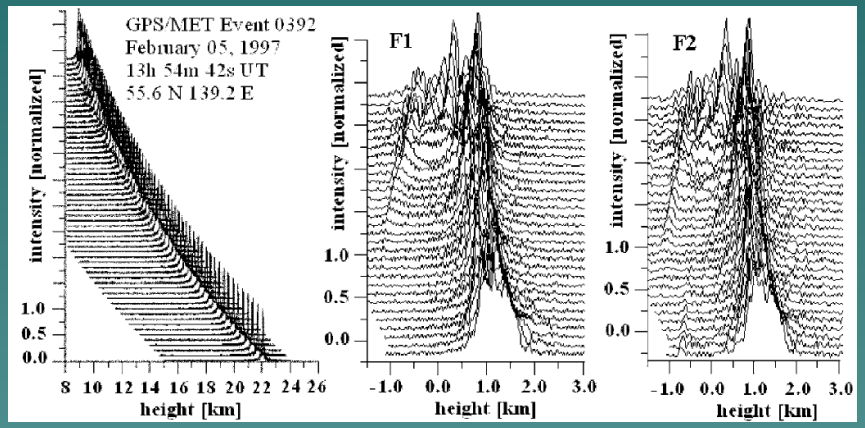

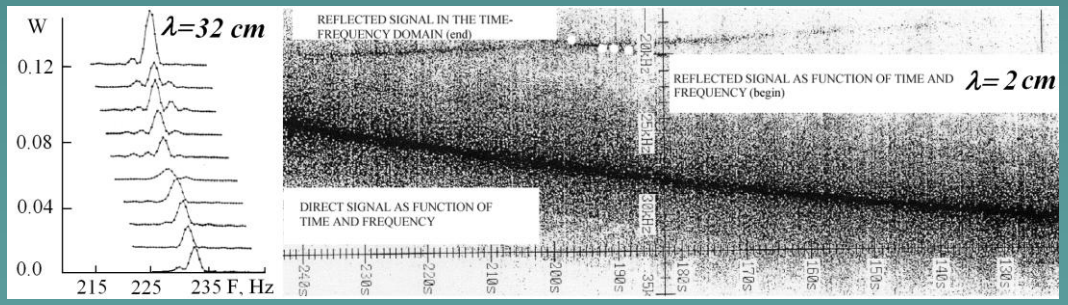

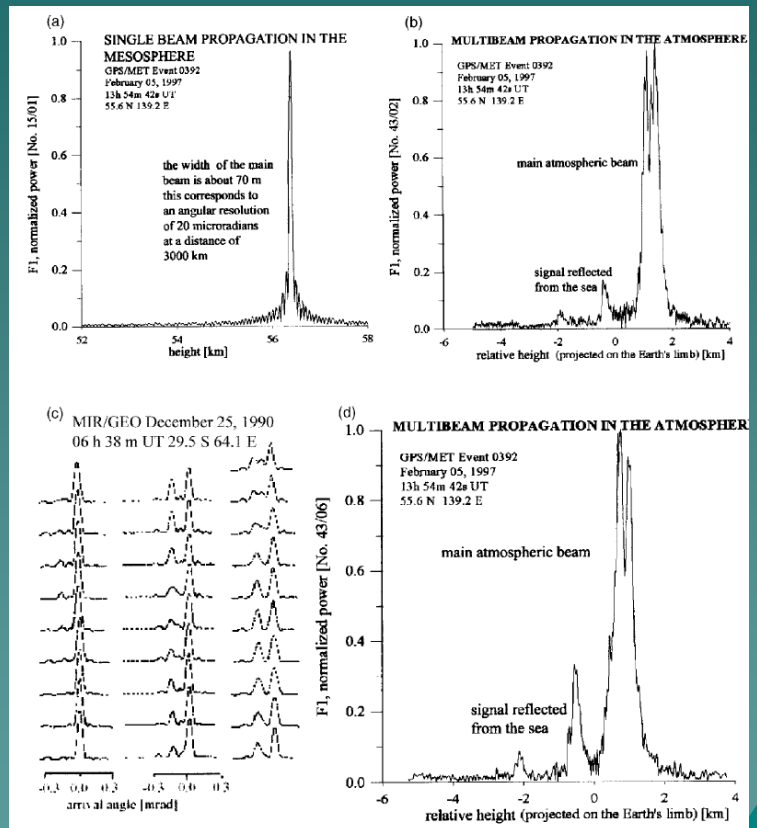

Figure 2. Radio brightness distribution in the Earth's atmosphere as seen from the LEO satellite. (a) Mesosphere, single-beam propagation, and a vertical resolution of about 70 m. (b–d) Signal that has been reflected from the sea and is well resolved relative to the main beam in the troposphere. The time interval between successive plots was about 0.48 s. Comparing the position of the reflected signal in neighboring plots shows the motion of the main beam.

Doppler shift of the reflection from the sea surface from data of MIR-GEO (λ=32 cm, right) (Pavelyev et al., 1996) . Model of the Doppler shift behavior (left).

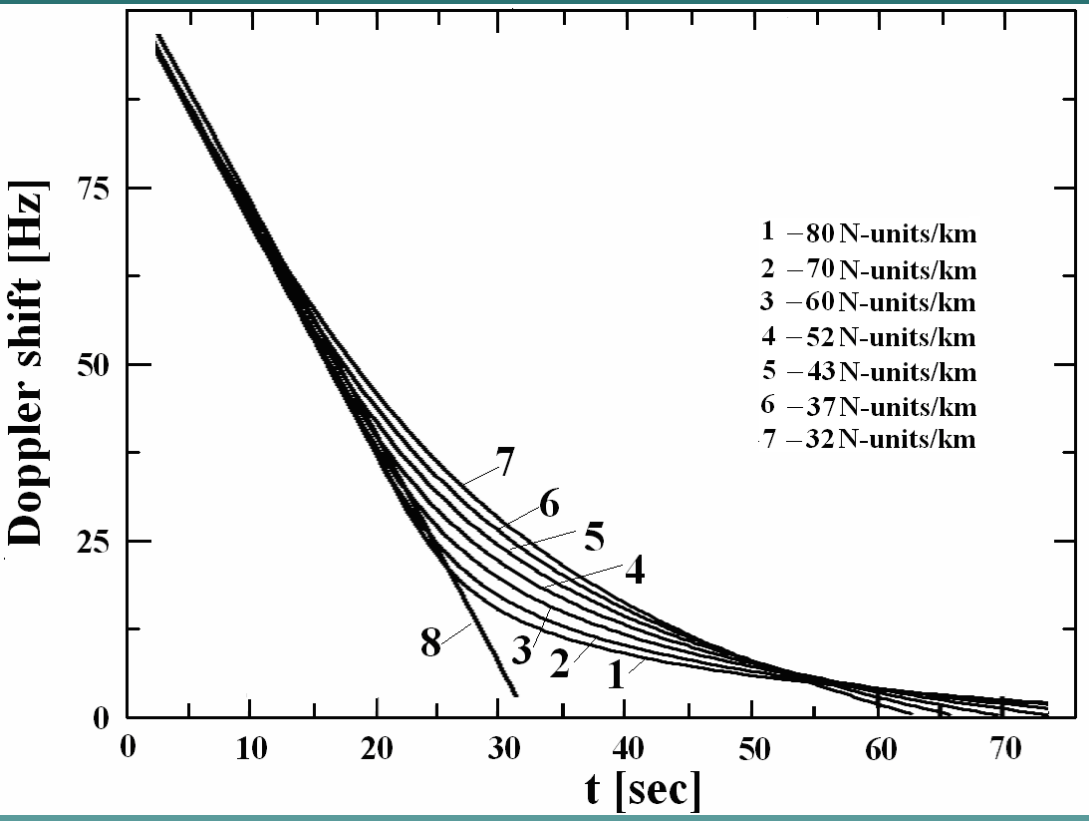

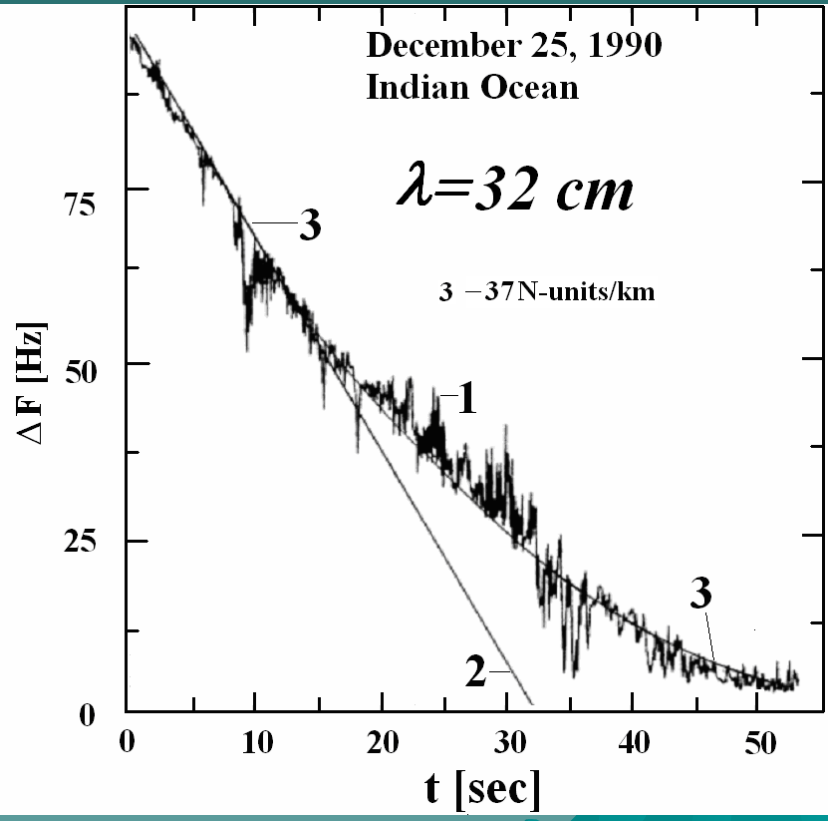

Reflection coefficient from data of MIR-GEO (right) at the 31.2° South latitude 68.2° East longitude (Pavelyev et al., 1996). Curves 1-3 correspond to N_0=320 N-units and dN/dh= –42 N-units/km. Curves 1,2,3, and 4 correspond to the sea surface conductivity 2.7, 4, and 7 mhos/m. Curve 4 correspond to the absence of the atmosphere. Curve 5 (4 mhos/m) accounts for the total absorption in the atmospheric oxygen. Model of the reflection coefficient (left). Curves 2-5 correspond to dN/dh=–35.4; –43.0; –50.0; – 57.0 N-units/km.

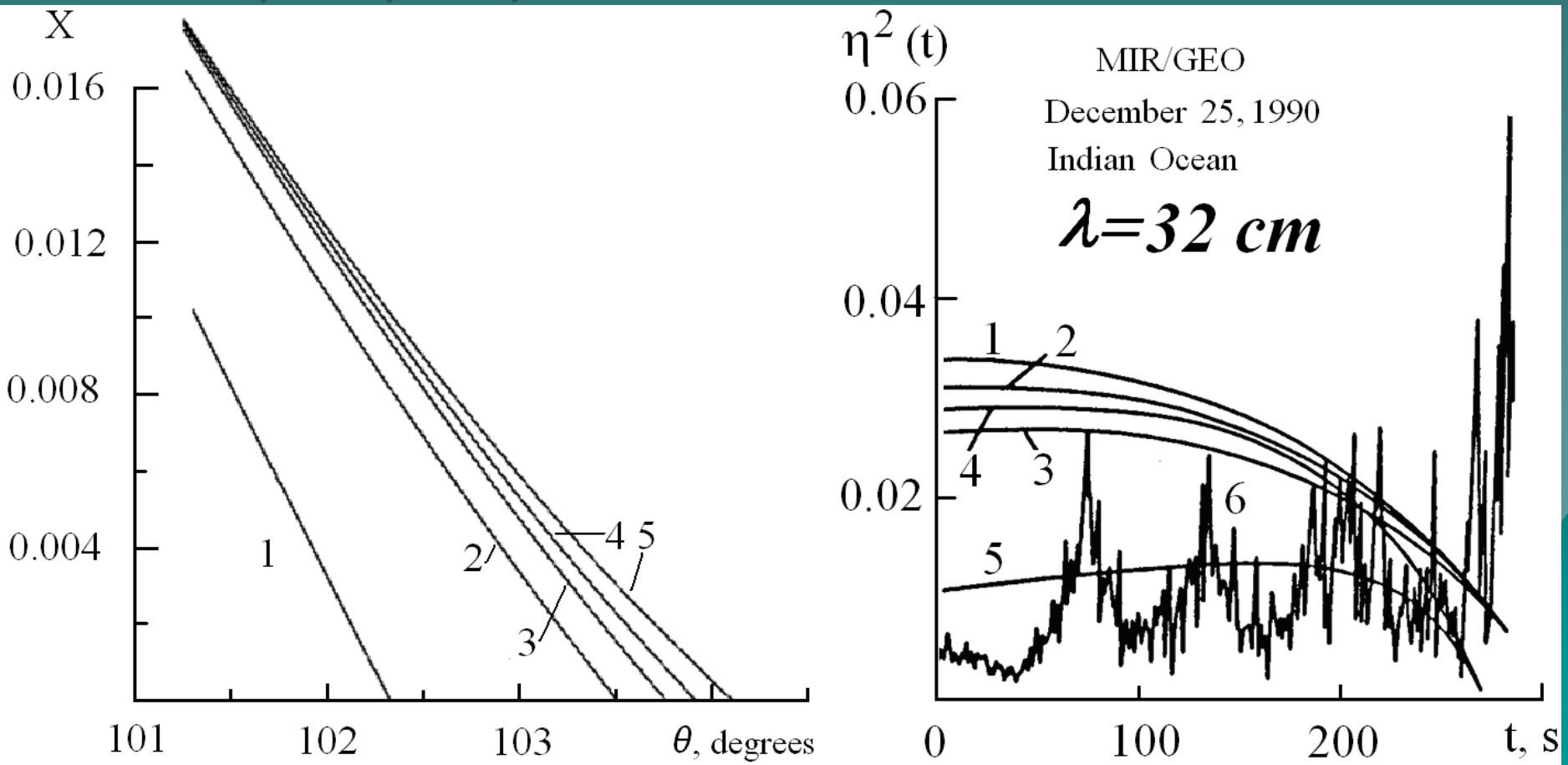

Conclusion

(i) The relationship between the Doppler shifts, eikonal acceleration, and refractive attenuations established earlier for the direct signals is valid for the reflected signals. This connection allows for recalculating the Doppler frequency (or the phase delay) of the reflected signals to the refractive attenuation (reflectivity cross-section) and opens a new possibility to measure the total absorption in the atmosphere at low elevation angles.

(ii)The introduced analytical model can be used for determining the fundamental characteristics of bistatic remote sensing with high accuracy including the phase delay, reflectivity cross-section, and Doppler shift with accounting for the refraction and absorption effects.

(iii) The derivative of the difference of the Doppler frequencies with respect to time is proportional to the difference of the refractive attenuation of the reflected and direct signals. These results are in a good agreement with the measurements data obtained during the MIR/GEO (wavelengths 2 and 32 cm), GPS/MET and CHAMP (wavelengths 19 and 24 cm) radio occultation experiments.

(iv) Detecting the reflected signals in radio occultation data can open new avenues for bistatic radio-holographic monitoring of the Earth's surface at low elevation angles.

(v)Experimental observation of the propagation effects at low elevation angles has also principal importance for fundamental theory of radio waves propagation.

Acknowledgements

We are grateful to GFZ-Potsdam for access to the CHAMP RO data. This research is supported through an Australian Research Council project (ARC- LP0883288) and the Department of Industry, Innovation, Science and Research of Australia International Science Linkage projects (DIISR/ISL-CG130127) and Australian Space Research Program. Work has been partly supported through grant № 10-02-01015-a, Russian Fund of Basic Research, and by program OFN-15 of Russian Academy of Sciences.

Thank you for your attention!